Journal of Thermal Analysis and Calorimetry
https://doi.org/10.1007/s10973-024-13333-y

Effect of alkyl chain length on the thermal properties and toxicity of *n*-alkyl-ammonium nitrate ionic liquids (*n* = 2, 3, 4, 5, 6, 8) for energy applications

M. Villanueva[1] · P. Vallet[1] · T. Teijeira[1] · A. Santiago-Alonso[1] · A. Amigo[2] · E. Tojo[3] · L. M. Varela[1] · J. J. Parajó[1] · J. Salgado[1]

Received: 2 November 2023 / Accepted: 19 May 2024

Abstract
The most currently used ionic liquids (ILs) are protic ionic liquids (PILs), subject to extensive investigation regarding their physical properties. These compounds along with their mixtures with other substances such as salts and solvents, serve as electrolytes in next generation electrochemical smart devices, and emerge as viable candidates to replace conventional Heat Transfer Fluids (HTFs) in various energy applications. Despite the extensive number of studies, important information about this kind of compounds is still unknown, such as the effect of alkyl chain length on thermal and thermophysical properties, as well as toxicity. This work, extending previous studies of our group, summarizes the liquid range, heat capacity and acute toxicity level of six ammonium ILs: specifically, *n*-alkyl-ammonium nitrate ILs with increasing alkyl chain length (*n* = 2, 3, 4, 5, 6, 8). For this study, the synthesis of the three ILs with the longest alkyl chain was performed, along with DSC, TGA and toxicity measurements. It was observed that an increase in alkyl chain length resulted in a decrease in short-term thermal stability and an increase in melting temperature, indicating a reduction in the liquid range. A compensation effect between enthalpy and entropy of melting was observed for the studied chain lengths. The isobaric specific and molar heat capacities increase with temperature for all the compounds studied here, and good correlations were obtained between molar heat capacity and the number of carbon atoms in the alkyl chain for every temperature. Finally, most of the ILs are non-toxic, although toxicity increases with alkyl chain length.

Keywords Ionic liquids · Thermal properties · Ecotoxicity · Transport properties

Introduction

Although the field of ionic liquids (ILs) started began more than a century ago, had long periods of insignificance during the twentieth century, but in recent decades has taken great importance [1]. ILs are widely defined as ionic materials, in the sense that have been formed for cations and anions with low melting points, lower than 100ºC, without any physical or chemical sense attached to this temperature. These conformational characteristics lead that these compounds have very interesting properties, such as their high chemical stability and their high miscibility with other solvents [2]. But the most identifying properties are its low, almost zero, vapour pressure and the possibility of modifying its properties by introducing functional groups into the most apolar part of its structure, which is known as the ability of tunning these compounds. For this reason, the applicability of the ionic liquids has increased enormously in the last decades,

✉ M. Villanueva
maria.villanueva@usc.es

J. J. Parajó
juanjose.parajo@usc.es

[1] Grupo de Nanomateriais, Fotónica e Materia Branda, Departamentos de Física Aplicada y Física de Partículas, Universidade de Santiago de Compostela, Campus Vida s/n, 15782 Santiago de Compostela, Spain

[2] Grupo de Propiedades Termofísicas e Superficiais de Líquidos, Departamento de Física Aplicada, Universidade de Santiago de Compostela, Campus Vida s/n, 15782 Santiago de Compostela, Spain

[3] Department of Organic Chemistry, Universidade de Vigo, Marcosende, Vigo, Spain

Published online: 22 June 2024

being now used in various fields, such as solvents, catalysers, electrolytes, heat transfer fluids (HTFs), lubricant bases and absorbents in heating pumps [3–7]. However, this tunability becomes a great challenge since the combinations of cations and anions that can form an IL are almost unlimited [8]. Therefore, it is crucial to understand, for example, how the alkyl chain length and different functional groups determine the IL properties.

Two subcategories of ILs can be found, protic (PILs) and aprotic (APILs) ILs. The key properties that distinguish PILs from other ILs are the proton transfer from the acid to the base, resulting in the presence of proton-donor and -acceptor sites. These sites can be used to build up a hydrogen-bonded network, leading to important properties such as low viscosity and high-water solubility [9] and lower toxicity [10]. The synthesis of PILs requires a simple equimolar acid–base reaction followed by drying, making PILs frequently the simplest and most economical to synthesize. Alkylammonium nitrates fall within this subcategory.

Despite the large number of papers investigating the properties and applications of the ILs, significant gaps remain for understanding their behaviour specially for PILs [8] because they have, in general, better transport properties and biodegradability, as well as being simpler and less expensive to synthesize [11, 12]. Among the knowledge gaps of PILs, it is crucial to characterize the changes that occur in different thermophysical properties based on the cation alkyl chain, enabling the rational design of PILs for specific applications.

Furthermore, taking in mind that toxicity is also an important parameter when selecting a material for industrial applications. ILs have an inherent reputation as environmentally friendly solvents due to their negligible vapour pressure, although low volatility does not completely eliminate the potential environmental hazards, and their water solubility could be a real concern. It has also been observed that an increase in alkyl chain length, or lipophilicity, is associated with higher degradation rates and increased toxicity [13]. Mutalib and Grahem [14] in their review, indicate that alkyl chain length appears to be the dominant parameter controlling the toxicity of ILs towards different aquatic organisms, including *Aliivibrio Fischeri* (*A. Fischeri*) and other trophic organisms. These authors carried out a comprehensive study of numerous families of ILs with different anions and cations, but PILs as common as alkylammonium nitrates were not included in their research.

The aim of this work was to complete the thermophysical characterization of alkylammonium nitrate ILs, initiated in a previous work with ethyl-, *n*-propyl and *n*-butyl-ammonium nitrate (EAN, PAN and BAN, respectively) [15]. For this purpose, the thermal behaviour and heat capacity of *n*-pentyl, *n*-hexyl- and *n*-octylammonium nitrate, (PEAN, HEAN and OAN), are reported and compared with those obtained for EAN, PAN and BAN, aiming to properly establish the effect of the cation alkyl chain length on these physicochemical properties.

Furthermore this study aims to also provide a complete characterization of the acute toxicity, in terms of bioluminescence variation of the marine bacterium *A. Fischeri* of *n*-alkylammonium nitrate ILs ($n = 2, 3, 4, 5, 6, 8$).

Materials and Methods

Chemicals

N-amylamine (Acros Organics, ≥ 99%), N-hexylamine (Thermo Scientific Chemicals, 98%), N-octylamine (Sigma-Aldrich, 99%), *n*-Hexane (≥ 99%, Acros Organics) and Nitric acid (65% solution in water, Acros Organics) were used as received without any pre-treatment.

Synthesis

^{1}H and ^{13}C NMR spectra were recorded on a BRUKER ARX 4CO spectrometer at 400.1621 (1H) and 100.6314 (^{13}C) MHz, respectively. $CDCl_3$ (ACROS Organics, 99.6 + atom % D) was employed as deuterated solvent. Chemical shifts are quoted in parts per million (ppm) relative to the signals corresponding to the residual non-deuterated solvent ($CDCl_3$: δH = 7.26 ppm, δC = 77.16 ppm). ESI Mass spectra were recorded on a BRUKER FTMS APEXIII. The glass material employed in the synthetic reactions was dried in an oven at 333 K for 24 h before use.

Synthesis of *n*-Pentylammonium nitrate (PEAN). N-amylamine (45 mL, 0.3834 mol) and hexane (50 mL) were placed in a round bottom flask over an acetone/dry ice bath. Nitric acid (65% solution, 26.55 mL) was added drop wise. The solution was stirred at room temperature, and the formation of two layers was observed. Hexane was decanted, solvents were removed heating under low pressure and the resulting ionic liquid was dried heating at 50 ºC under high vacuum for 48 h. Pentylammonium nitrate (PEAN) was obtained as a colourless semisolid (56.46 g, 98%). RMN-^{1}H ($CDCl_3$, δ, 400 MHz): 7.44 (s, 3H, NH_3), 3.04 (m, 2H, CH_2NH_3), 1.70 (m, 2H, $CH_2CH_2NH_3$), 1.33 (m, 4H, $CH_2CH_2CH_2CH_2NH_3$), 0.88 (t, 3H, J = 7.0 Hz, $CH_3CH_2CH_2CH_2CH_2NH_3$). RMN-^{13}C ($CDCl_3$, δ, 100.6 MHz): 40.4, 28.4, 27.1, 22.1, 13.7. HRMS (ESI) *m/z* (%): found 88.1122 $[A]^+$ (100), calcd for $[C_5H_{14}N]^+$: 88.1126; found 238.2135 $[A_2B]^+$ (40), calcd for $[C_{10}H_{28}N_3O_3]^+$: 238.2131.

Synthesis of *n*-Hexylammonium nitrate (HEAN). N-hexylamine (89.40 mL, 0.67 mol) and hexane (100 mL) were placed in a round bottom flask over an acetone/dry ice bath. Nitric acid (65% solution, 46.40 mL) was added drop wise. The solution was stirred at room temperature, and the formation of two layers was observed. Hexane was decanted,

solvents were removed heating under low pressure and the resulting ionic liquid was dried heating at 50 ºC under vacuum for 48 h. Hexylammonium nitrate was obtained as a colourless semisolid (109.68 g, 99.7%). RMN-^{1}H ($CDCl_3$, δ, 400 MHz): 7.47 (s, 3H, N*H*$_3$), 3.06 (m, 2H, C*H*$_2$NH$_3$), 1.73 (*a*quint, $J = 7.6$, 2H, C*H*$_2$CH$_2$NH$_3$), 1.32 (m, 6H, (C*H*$_2$)$_3$(CH$_2$)$_2$NH$_3$), 0.89 (t, 3H, $J = 6.8$ Hz, C*H*$_3$(CH$_2$)$_5$NH$_3$). RMN-^{13}C ($CDCl_3$, δ, 100.6 MHz): 40.4, 31.2, 27.5, 26.1, 22.4, 13.9. HRMS (ESI) *m/z* (%): found 102.1278 $[M]^+$ (40), calcd for $[C_6H_{16}N]^+$: 102.1283; found 266.2440 $[A_2B]^+$ (100); calcd for $[C_{12}H_{32}N_3O_3]^+$: 266.2444.

Synthesis of *n*-Octylammonium nitrate (OAN). N-octylamine (96.45 mL, 0.58 mol) and hexane (100 mL) were placed in a round bottom flask over an acetone/dry ice bath. Nitric acid (65% solution, 40.0 mL) was added drop wise. The solution was stirred at room temperature, and the formation of two layers was observed. Hexane was decanted, solvents were removed heating under low pressure and the resulting ionic liquid was dried heating at 50 ºC under vacuum for 48 h. Octylammonium nitrate was obtained as a colourless semisolid (110.7 g, 99%). RMN-^{1}H ($CDCl_3$, δ, 400 MHz): 7.46 (s, 3H, N*H*$_3$), 3.03 (m, 2H, C*H*$_2$NH$_3$), 1.70 (m, 2H, C*H*$_2$CH$_2$NH$_3$), 1.26 (m, 10H, (C*H*$_2$)$_5$(CH$_2$)$_2$NH$_3$), 0.86 (t, 3H, $J = 6.9$ Hz, C*H*$_3$(CH$_2$)$_7$NH$_3$). RMN-^{13}C ($CDCl_3$, δ, 100.6 MHz): 40.4, 31.8, 29.2, 29.1, 27.6, 26.5 (*C*H$_2$(CH$_2$)$_5$NH$_3$), 22.6, 14.0. HRMS (ESI) *m/z* (%): found 130.1592 $[A]^+$ (100), calcd for $[C_8H_{20}N]^+$: 130.1596.

Phase transition determination

A differential scanning calorimeter DSC Q1000 from TA-Instruments was used to determine the different phase transitions experimented by the selected ILs during heating and cooling cycles. Samples, without further purification, were placed in a 40 µL hermetically sealed aluminium pan with a pinhole at the top of the cover. Each sample (3–5 mg) was subjected to four ramps, two in cooling and two in heating mode, with an isothermal step between them, following the same schedule than as that used in previous works [16, 17], which is essential for enabling comparison of the results obtained in the present work with those of previous studies. A previous isothermal step at 120 °C for 45 min was included to remove impurities (mainly water absorbed during the sample preparation) and erase the thermal history of the samples. Transitions temperatures were determined from the DSC curves, as the onset points of the different peaks, during the reheating and re-cooling steps. Temperature and heat of melting of indium were used for calibration [6, 17].

Thermogravimetric analysis

To study the short-term thermal stability and determine the higher temperature of the liquid range window, thermal stability of the selected ILs was performed. Experiments were carried out using a DSC/TGA1 instrument from Mettler Toledo in dynamic mode, with a heating rate of 10 K min^{-1} and a purge gas flow of 20 cm^3 min^{-1}, from (50 to 800) ºC under a N_2 atmosphere. Samples of 3–5 mg were placed in an open platinum pan [18, 19].

Heat capacity

Specific heat capacities were obtained using the isothermal step method with a Micro DSCIII differential scanning calorimeter from Setaram, France. Calibration was performed using a Joule effect calibration vessel (Setaram) and checked using *n*-decane and squalane (Sigma-Aldrich 99%) as heat capacity standards [20]. The background noise of the Micro DSCIII was less than 3 µW. Dynamic scans of samples of around 0.6 g were conducted at a heating rate of 0.25 K min^{-1} within the temperature range of (293.15–348.15) K. Squalene was used as the reference fluid to determine the heat capacity values due to its similar values of heat flow and the high precision of the available literature data [20]. Experiments followed the experimental technique and procedure previously described [21, 22]. The standard uncertainty in C_p experimental values is estimated to be 0.002 J·g^{-1}·K^{-1}.

Toxicity

The toxicity of the six ILs ($C_nNH_3NO_3$; $n = 3$, 4, 5, 6 and 8) was assessed using the Microtox® Toxicity Test kit following the same procedure detailed elsewhere [23, 24]. The Microtox® Toxicity test evaluates the luminescence inhibition of the Gram-negative marine bacteria *Aliivibrio Fischeri* (*A. Fischeri*) through a population-dependent mechanism called quorum sensing sensitive. It considers that exposure to a toxic substance disrupts the respiration of the bacteria, being the with luminescence production being directly proportional to the metabolic activity of the bacterial population. The results here obtained were completed with those previously obtained for the IL with the shortest alkyl chain length, EAN [24].

A series of diluted aqueous solutions (from 0 to 81.9%) of each IL was prepared for the acute toxicity test. Various exposure times (5, 15 and 30 min) to the IL were analysed. These data were used to estimate the effective concentrations that promote 50%, 20% and 10% (EC_{50}, EC_{20} and EC_{10}, respectively) of luminescence inhibition, and the corresponding 95% confidence intervals through a non-linear regression, using the least-squares method to fit the data to the logistic equation [23].

Results and discussion

Synthesis

The synthesis of the selected ILs *n*-pentyl-, *n*-hexyl- and *n*-octylammonium nitrate (PEAN, HEAN, OAN) was carried out through a neutralization reaction of the precursor BrØnsted acid/base pair using stoichiometric ratios of the acid (nitric acid) and the base (the corresponding *n*-alkylamine), following a procedure previously described [25]. Their structures were determined by ^{1}H and ^{13}C NMR, as well as High Resolution Mass Spectra, and in the case of PEAN, confirmed by comparison with the NMR data previously described [26]. Spectra are provided in the ESI (figures S1-S3). From the NMR spectra a purity ≥ 99 mass% was estimated for the three synthesized ILs, determined using the following equation, where *I* represents the relative area of each signal: [27]

$$Purity\% = \left[\frac{\sum I_{\text{product}}}{\sum I_{\text{total}}}\right] \cdot 100$$

The ESI mass spectra of the synthesized *n*-alkylammonium nitrate ILs showed the formation of the typical ILs cluster ions of the type $[A_2B]^+$, where A = cation and B = anion. To our knowledge, no NMR or Mass spectra have been previously published for HEAN and OAN. The chemical structures and purities of the synthesized ILs are shown in Table 1.

Liquid range

The liquid range is the temperature interval between melting and thermal degradation temperatures.

DSC phase transition analysis

In Fig. 1, the DSC curves obtained for the synthesized ILs, PEAN (a), HEAN (b) and OAN (c), in heating and cooling ramps are shown. Table 2 summarizes the thermal transitions obtained from DSC curves of the three ILs in cooling and heating ramps. Results for EAN [6], PAN and BAN [15]

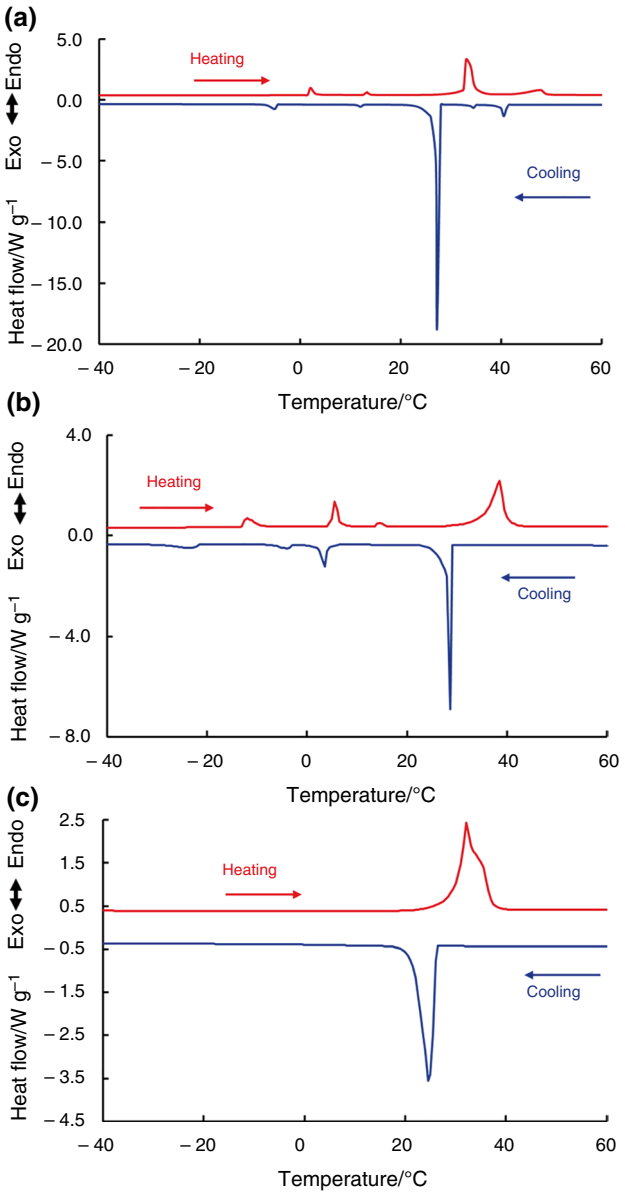

Fig. 1 DSC curves on heating and cooling ramps for **a** PEAN, **b** HEAN and **c** OAN ILs

Table 1 Structure, abbreviations, and purity of the selected ILs

Name	Abbreviation	Chemical structure	Molecular mass / g·mol^{-1}	Purity/ mass%
n-Penthylammonium nitrate	PEAN $C_5H_{14}N_2O_3$	$^{+}H_3N$ ~ NO_3^-	150.18	≥ 99
n-Hexylammonium nitrate	HEAN $C_6H_{16}N_2O_3$	$^{+}H_3N$ ~ NO_3^-	164.20	≥ 99
n-Octylammonium nitrate	OAN $C_8H_{20}N_2O_3$	$^{+}H_3N$ ~ NO_3^-	192.25	≥ 99

Table 2 Onset temperature, enthalpy, and entropy of the main melting peak per gram and per mol of sample (t_m, $\Delta_m H$ and $\Delta_m S$), and onset temperature and enthalpy of the main freezing peak per gram of sample (t_f and $\Delta_f H$) obtained from DSC curves of the ILs. Onset temperature, peak temperature, and Wooster temperature (t_{onset}, t_{peak}, $t_{Wooster}$) obtained from dynamic TG and DTG curves. Experiments were performed under an atmospheric pressure of (1008 ± 10) hPa and a relative humidity of (55 ± 10)%

IL	t_f/ °C	t_m/ °C	$\Delta_f H$/ J g^{-1} h	$\Delta_m H$/ J g^{-1}	$\Delta_m H$/ kJ mol^{-1}	$\Delta_m S$/ J g^{-1} K^{-1}	$\Delta_m S$/ J mol^{-1} K^{-1}	t_{onset}/ °C	t_{peak}/ °C	$t_{Wooster}$ / °C [37]
EAN [6]	−27	12	76	122	13.2	0.43	46	248	260	108
PAN [15]	−28	5	61	71	8.6	0.25	31	244	255	107
BAN [15]	−6	40	55	126	17.1	0.40	55	235	244	115
PEAN	24	33	45	42	6.3	0.14	21	208	218	109
HEAN	28	36	42	42	6.7	0.13	22	183	215	108
OAN	26	30	64	63	11.4	0.20	38	178	191	80

Expanded uncertainties are U(t) = 6 °C and U$_r$(ΔH) = 4% (0.95 level of confidence (k = 2))

have been previously reported but, for a better comparison, they are also included in Table 2. As it can be seen, melting (endothermic peak in heating ramp) and freezing (exothermic peak in cooling ramp) transitions were found for the three ILs within the studied temperature range. It must be remarked that freezing temperatures are lower than melting, reflecting the characteristic supercooling effect typical in ILs [28, 29] However, the supercooled liquid region with increasing cation alkyl chain length, and virtually disappears for the longest chains studied. This supercooling effect tends to diminish and practically vanish with increasing carbon chain length.

From Fig. 1a, PEAN exhibits several small peaks in heating and cooling ramps, with a main endothermic peak in heating and an exothermic peak in cooling. These could all be associated with the melting of different crystalline forms, with the predominant form having an onset temperature of 33 ºC. As observed, there is concordance between the peaks in the cooling and heating curves, all of them exhibiting the aforementioned supercooling effect. Nevertheless, in the case of the peak observed at 40–50 ºC during heating, it splits into two peaks on the cooling scan. In order to check the dependence of the supercooling effect, values corresponding to the hysteresis for the six ILs are presented in the ESI file in Table S1. For HEAN (Fig. 1b), a similar behaviour is observed, with the peak onset at 36 ºC corresponding to the main melting process. PEAN and HEAN are polymorphic ILs [30], but OAN (Fig. 1c), with a single peak upon heating and a single peak upon cooling, does not present this behaviour. To the best of our knowledge, no similar previous results for these ILs have been reported. Figure 2a shows the melting temperature of *n*-alkyl-ammonium nitrate ILs in terms of the number of carbon atoms in the cation alkyl chain length (n = 2, 3, 4, 5, 6, 8). PAN exhibits the lowest melting temperature, while BAN the highest, indicating that the odd and even numbers of alkyl chain groups present different behaviour, as previously pointed out by Rodrigues & Santos [31] who attributed it to the contribution of the

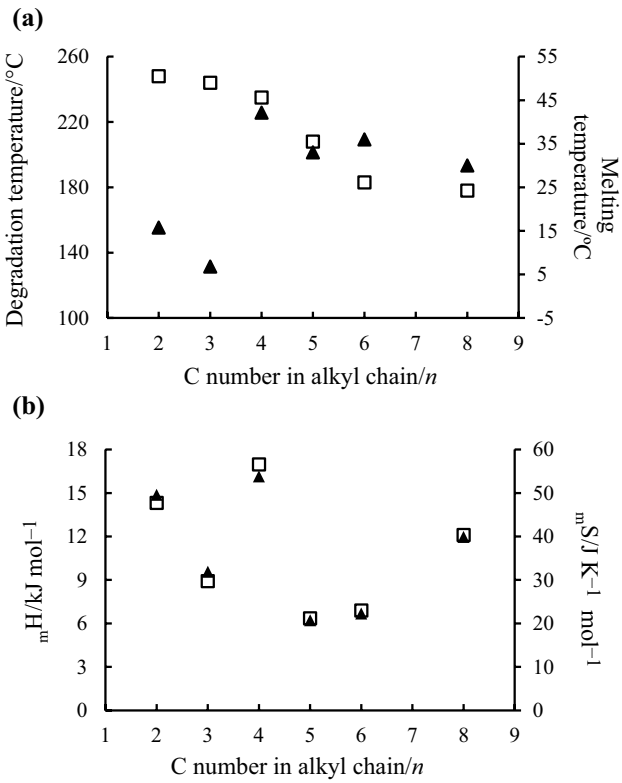

Fig. 2 Cation chain length (n) dependence of **a** onset degradation and onset melting temperatures obtained from TGA and DSC experiments, respectively, and **b** enthalpy and entropy of fusion

alkyl chain to the stability of crystal packing. As seen in Table 2, the melting point does notdirectly correlate with the alkyl chain length, as previously observed for pyrrolidinium-based ILs [32]. Greaves & Drummond [33] noted in their interesting review that most of the alkylammonium nitrate compounds are considered as high temperature molten salts, given that their melting points exceed 100 ºC. However, all six alkylammonium nitrate ILs studied here exhibit melting temperatures below that temperature threshold. This

contradiction could be explained by the fact that Greaves & Drummond analysed the melting temperature of twelve ammonium nitrates with different alkyl groups (aromatic, ester, and ramified groups), whereas in the present work, the ammonium compounds differ only in the length of the cation alkyl chain. The use of different alkyl groups results in varying cation–anion intermolecular forces in the PIL, which affect the melting point [34].

The melting point of ILs is strongly related to the strength of the crystal lattice, which, in turn, is determined by intermolecular forces, molecular symmetry, and conformational degrees of freedom, that is by the packing efficiency. Bagno et al. [35] have suggested that in the case of ILs packing inefficiency, low melting points are observed [31]. In our case, although the melting points are lower than 100 ºC, only EAN and PAN are really room temperature ionic liquids (RTILs). Then, the highest packing efficiency corresponds to BAN, and increasing the alkyl chain length from it results in a decrease in the packing efficiency and a decrease in the H-bond fraction. Additionally, PEAN, HEAN and OAN show lower values of melting enthalpy and entropy compared to EAN, PAN and BAN, despite their high molecular mass. This, coupled with the numerous additional transitions observed in their DSC profiles, confirms the difficulty to of finding a stable crystal form and behaviour closer to a plastic crystal, as indicated by Timmermans' criterium [6, 36].

Figure 2b shows a similar trend for molar enthalpy and for molar entropy with respect to the carbon number of the alkyl chain.

Thermal stability

The thermal stability of the new three synthesized ILs has been analysed through thermogravimetry, in dynamic mode at a heating rate of 10 K min^{-1}, and under N_2 atmosphere. The thermal stability of EAN [6], PAN and BAN [15] has also been previously studied and reported, and it was considered for better comparison. All ILs show a unique step in thermogravimetric curve. Onset temperatures, t_{onset}, percentual remaining mass, W_{onset}, temperature at 90% of remaining mass $t_{10\%}$ and temperature of the minimum of DTG, t_{peak}, were determined following the criterion indicated in previous works [6, 16]. Table 2 also shows the onset and peak temperatures, while the other parameters can be found in Supplementary material (Table S2). In the ESI file a comparison of the TG curves obtained for the six ammonium ILs has been included (Fig S6). A clear dependence on the alkyl chain length is observed in the three temperatures, onset (see Fig. 2a) and peak temperatures, and temperature at 10% of mass loss, all of which decrease with the number of carbon atoms. Considering these temperatures, the following trend can be stated related to thermal stability:

EAN > PAN > BAN > PEAN > HEAN > OAN.

In the same way as for temperature of the thermal transitions, to our knowledge, no references can be found in the literature for these parameters for the ILs PEAN, HEAN and OAN.

As it is well known, the criterion based on the onset degradation temperature is a useful for comparative analysis between different materials, but it tends to overestimate long-term thermal stability. For this reason, many authors use the method proposed by Wooster et al. [37] which is more rigorous. They suggested that the temperature at which 1% degradation occurs in 10 h ($t_{0.01/10\,h}$) is a reliable indicator of thermal stability. Furthermore, Wooster et al. [37] established a method to estimate $T_{Wooster}$, expressed in Kelvin, from dynamic scans using the equation:

$$T_{Wooster} = 0.82T_{(dW/dt\neq 0)}$$

being $T_{(dW/dt\neq 0)}$ the temperature in Kelvin at which the first appreciable mass loss occurs. The results of this calculation are also shown in Table 2. As expected, the values obtained are much lower than the onset temperature. This seemingly contradictory difference needs to be clarified: Wooster criterion is related to isothermal study conditions, while the onset temperature is determined under dynamic conditions. This implies that, for long-term exposure, the Wooster criterion is mandatory, whereas for short-term exposure, the stability limit can be extendedup to the onset temperature.

Finally, the liquid range of these ILs, calculated as the difference between the onset degradation temperature (if the IL is exposed to high temperatures for a short time) or Wooster temperature (for applications requiring prolonged high temperatures) and the main melting temperatures, was determined and presented in Table 3. The liquid range decreases with the alkyl chain length, although it appears to exhibit an asymptotic tendency for the highest carbon numbers. This observation is in agreement with the assumption proposed by Serra et al. [38] which suggests the existence of a critical alkyl size (CAS). Beyond this point, further increase in the alkyl chain length does not significantly change the interaction within the polar

Table 3 Liquid range of the selected PILs

IL	Short-term t_{onset}—$t_{melting}$ /°C	Long term $t_{Wooster}$—$t_{melting}$ /°C
EAN	236	96
PAN	242	102
BAN	195	75
PEAN	175	76
HEAN	147	72
OAN	148	50

network (anion-cation) or the structural organization of the ILs in the crystal.

Heat capacity analysis

The specific (c_p) and molar (C_p) heat capacities in the liquid phase, between (310.15 and 348.15) K, for PEAN, HEAN and OAN ILs are available as supporting information (Table S3). For a complete comparison, the specific heat capacity of the six ammonium ILs (EAN, PAN, BAN, PEAN, HEAN and OAN) is presented in Fig. S4. For all six ILs, c_p increases with temperature as expected, and with the alkyl chain length, although a clear tendency with n cannot be found.

The isobaric molar heat capacity values, C_p, for these ILs are plotted against temperature in their liquid range (310.15- 348.15) K in Fig. 3. C_p often correlates with molar mass since the degrees of freedom of the molecule strongly increase with its size [39]. As stated Fredlake et al.[40], the greater the molar mass, the greater the molar heat capacity.

A second-degree polynomial equation has been used to fit the molar heat capacity against temperature. The fitting parameters, along with the values of the absolute average percentage deviation (AAD%), the maximum percentage deviation (DMAX%), and the average percentage deviation (Bias%) [41] are displayed in Table 4.

A good linear correlation between molar heat capacity and the carbons number (n) of the alkyl chain for all the temperatures was found, as can be observed in Fig. 4 and Figure S5, which show the molar heat capacity versus n for two temperatures (313.15 K, and 343.15 K) and for the rest of temperatures studied, respectively. The fitting parameters are shown in Table 5. This linear tendency agrees with the findings of Serra et al. [38], observed in a family of $[C_nC_1im][PF_6]$ ILs and Rocha et al. [42] in the $[C_nC_1im][NTf_2]$ IL series. For the ammonium ILs studied in the present work, a slope value of (32.3±0.7) J mol^{-1} K^{-1} was obtained for the linear relationship between molar heat capacity and the number of carbons, at 313.15 K. This value at each temperature represents the contribution of the CH_2 group to C_p at this temperature [43]. The obtained values range between 32.2 and 33.7 J mol^{-1} K^{-1}, show good concordance with those obtained by Serra et al. [38] for $[C_nC_1im][PF_6]$ at 298.15 K, with n = 2–10, 12, (32.1±0.5) J mol^{-1} K^{-1}, using a Setaram μDSC III microcalorimeter.

With the aim to compare the slope of the fitting and the CH_2 contribution each temperature, the group contribution method introduced by Gardas & Coutinho [43] was used to estimate the role of this functional group in the molar heat capacity, obtaining the following equation:

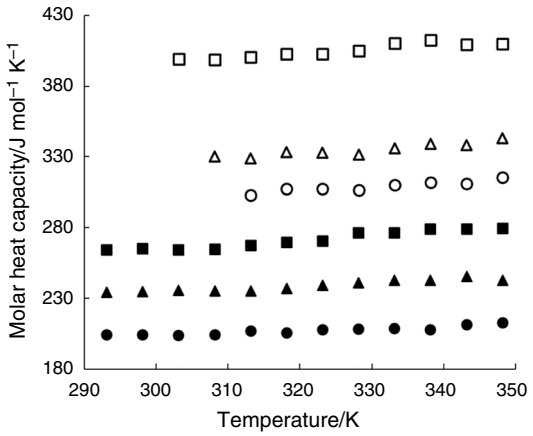

Fig. 3 Comparisons of isobaric molar heat capacity for the six ILs: ●EAN, ▲PAN, ■BAN, ◌PEAN, △ HEAN and OAN. Experiments were performed at (978 ± 5) hPa of atmospheric pressure. Values for EAN, PAN and BAN are reproduced from ref [15]

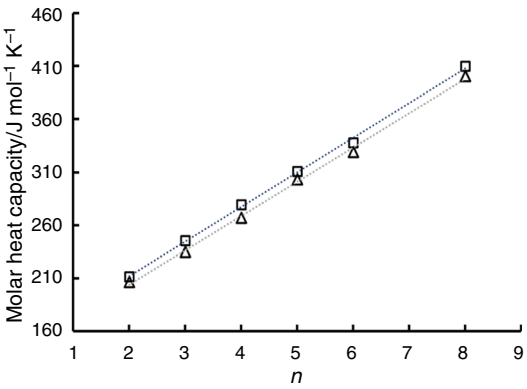

Fig. 4 Molar heat capacity, C_p, of a function of the number of carbon atoms in the alkyl side chain of the cation, n at 313 K and 343 K

Table 4 Parameters obtained from a fitting of experimental molar heat capacity values to a second-degree polynomial equation. $C_p = a + bT + cT^2$ and AAD%, DMAX% and Bias%

IL	a /J mol^{-1} K^{-1}	b /J mol^{-1} K^{-2}	c /J mol^{-1} K^{-3}	AAD%	DMAX %	Bias %
EAN	368.13	−1.16	0.002	0.3013	0.0104	0.0082
PAN	571.02	−2.33	0.004	0.2471	0.0051	−0.0023
BAN	906.72	−4.40	0.008	0.6016	0.0291	−0.3583
PEAN	450.01	−1.15	0.002	0.3901	0.0061	0.0157
HEAN	959.15	−4.12	0.007	0.3898	0.0068	0.0681
OAN	92.78	1.61	−0.0020	0.3790	0.0083	−0.0562

Table 5 Parameters and correlation coefficients obtained from the linear fitting $Cp = a + b \cdot n$, between molar heat capacity and carbon numbers at each temperature (Fig S5) and estimated values of molar heat capacity corresponding to the CH_2 group, $C_{P,\,CH2}$, using the group contribution method of Gardas and Coutinho [43]

T /K	a ± s(a)/ J mol^{-1} K^{-1}	b ± s(b)/J mol^{-1} K^{-1}	R^2	$C_{P,\,CH2}$ /J mol^{-1} K^{-1}
313.15	139.6 ± 3.4	32.3 ± 0.7	0.997	33.07
318.15	139.5 ± 2.7	32.8 ± 0.5	0.998	33.40
323.15	142.3 ± 2.8	32.9 ± 0.5	0.999	33.73
328.15	144.2 ± 4.0	32.2 ± 0.8	0.997	34.04
333.15	142.6 ± 3.4	33.1 ± 0.7	0.998	34.35
338.15	141.5 ± 3.2	33.7 ± 0.6	0.998	34.64
343.15	146.9 ± 2.8	32.6 ± 0.6	0.998	34.92

$$C_{CH_2} = R\left[-1.133 + 2.443\left(\frac{T}{100}\right) - 0.259\left(\frac{T}{100}\right)^2\right]$$

where R is the gas constant and T the absolute temperature.

Results for each temperature are included in Table 5, showing a very good agreement between them and the slopes obtained.

As seen in Fig. 4 and Table S3, the highest molar heat capacity value for all the PILs analysed here was 412 J·mol^{-1}·K^{-1}, corresponds to the ammonium IL with the longest cation alkyl chain (OAN). This value is not particularly high compared to other ILs, and it is in agreement with the observation of Liaqat et al. [44], who states that ammonium ILs are those with the lowest average heat capacity among all cation types present in the NIST ILThermo data base [45], 375 J·mol^{-1}·K^{-1} versus 315 J·mol^{-1}·K^{-1}, calculated here as the average value for the PILs analysed at the highest temperature [36].

Toxicity

Effective concentration value (EC_{50}) and the respective 95% confidence intervals at the three selected times are exposed in Table 6 for all the studied compounds; in the case of ethylammonium nitrate, previously published results were used [24]. EC_{20} and EC_{10} values for the six ILs are shown in supplementary information (Table S4 and Table S5, respectively).

As previously reported [46], the toxicity of the IL increases with length of the alkyl chain. This behaviour is related to the higher lipophilicity of long alkyl chain length, probably facilitating the entrance of the IL through the cell membrane. It also can be seen that the "cut-off" effect [47] does not appeared; this phenomenon suggests that toxicity reaches a maximum level at a certain chain length. In the case of the studied alkyl chain lengths, this maximum toxicity level has not been reached. To visualize this tendency with respect to carbon number, a bar graphic of EC_{50}, EC_{20} and EC_{10} at 5, 15 and 30 min is shown in Fig. 5.

Considering the EC and TU values of the studied compounds, most of the ILs studied exhibit a lower toxicity compared to those previously reported. The EC_{50} at 15 min of C_4C_1pyrr TFSI is less than 1000 mg L^{-1}, $C_4C_1C_1$im TFSI is very close to 100 mg L^{-1} [48, 49], or even choline- and betaine-based ILs, usually associated with more environmentally friendly ILs, present values between 10 and 1000 mg L^{-1} [23, 50]. In the present study, the toxicity values are higher than 1000 mg L^{-1} (considered non-toxic) from C_2 to C_5 alkyl chain length, and only the case of C_8 can be considered toxic.

The increase in toxicity with increasing alkyl chain length, as reported by other authors [51, 52] can be seen in Fig. 5 [51, 52]. Although different studies suggest that the anion is the main key parameter in toxicity [53, 54], our findings indicate that the influence of the cationic structure must be taken into consideration, as previously pointed out other authors [47, 55].

Conclusions

Three nitrate ILs derived from *n*-alkylammonium cations of long alkyl chain length ($n = 5, 6, 8$) were synthesized and their thermophysical properties were compared to those of the three others ILs of the same family with shorter alkyl

Table 6 EC_{50} effective concentration values in mg·L^{-1} and the respective 95% confidence intervals, for the three exposure times of the marine bacteria *A. Fischeri*

Compound	EC_{50}(5 min)/mg L^{-1}	EC_{50}(15 min)/mg L^{-1}	EC_{50}(30 min)/mg L^{-1}
EAN [24]	12,582.07 (8186.64; 16,977.50)	10,665.47 (6650.14; 14,680.80)	9711.63 (6561.46; 12,860.79)
PAN	8314.99 (7268.61; 9361.37)	5932.88 (5043.45; 6822.30)	5827.78 (4998.72; 6656.84)
BAN	1491.986 (636.69; 2347.04)	1066.71 (551.52; 1581.90)	1017.14 (478.49; 1555.78)
PEAN	1116.93 (945.07; 1222.79)	1073.63 (836.26; 1311.00)	1029.81 (792.52; 1267.11)
HEAN	85.69 (77.71; 93.68)	57.54 (52.98; 62.09)	50.11 (44.85; 55.39)
OAN	9.70 (6.37; 13.03)	7.33 (5.23; 9.43)	7.38 (5.51; 9.25)

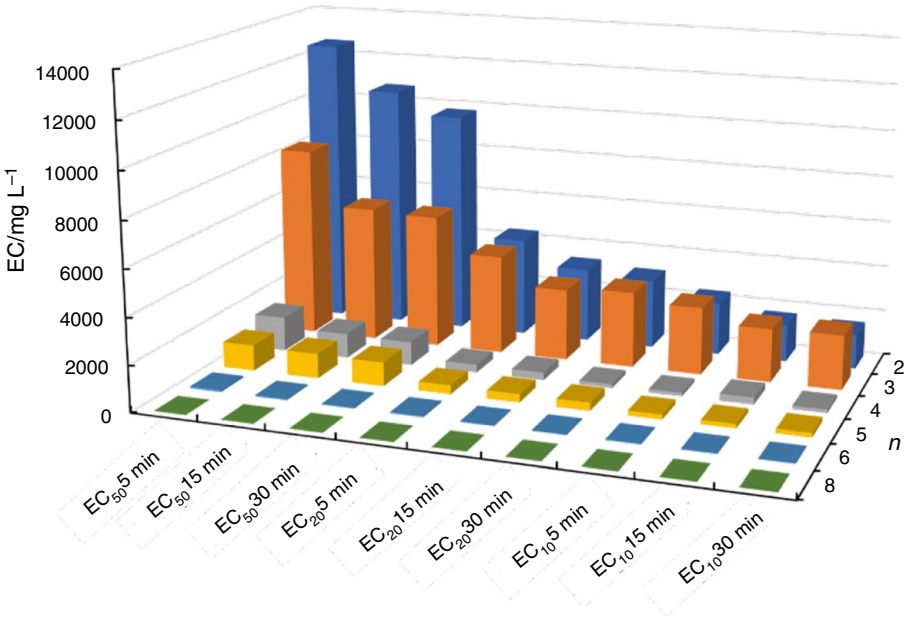

Fig. 5 Bar graphic of EC_{50}, EC_{20} and EC_{10} after 5, 15 and 30 min of exposure in terms of carbon number, *n*

chain length ($n = 2, 3, 4$) that were previously studied. The main conclusions are as follows:

- The akyl chain length decreases the short-term thermal stability, with this change being more significant for longer chain ILs.
- The melting temperature changes with the alkyl chain length, but there is not a clear tendency with the carbon number. It can be inferred that there are two different trends for even or odd carbon atoms, as observed by other authors in other ILs families.
- Because of the above results, the liquid range of these ILs decreases with the alkyl chain length.
- Isobaric specific and molar heat capacities of the six PILs increase with temperature as expected. Second-degree polynomial equations were found to correlate molar heat capacities and temperature.
- Isobaric specific and molar heat capacities increase with the number of carbon atoms in the cation alkyl chain. Good correlations were obtained between the molar heat capacity and the number of carbon atoms in the cation alkyl chain for each temperature, with the slope of the linear fitting representing the contribution of CH_2 group to the C_p at each temperature.
- The general trend indicates that IL toxicity increases with alkyl chain length, as reported by other authors for various families of ILs. This is likely due to the increase in cation lipophilicity caused by longer alkyl chains, which facilitates IL penetration through the cell membrane.

Acknowledgements Authors acknowledge M. Gómez (RIAIDT-USC) for the technical support in DSC and TGA measurements. This work was supported by Spanish Ministry of Economy and Competitiveness and FEDER Program through the projects MAT2017-89239-C2-1-P, PID2020-112846RB-C22 as well as by Xunta de Galicia through GRC ED431C 2020/10 project and the Galician Network of Ionic Liquids (ReGaLIs) ED431D 2017/06. P. Vallet thanks funding support of FPI Program from Spanish Ministry of Science, A. Santiago thanks funding to Doutoramento industrial program from GAIN-Xunta de Galicia and J. J. Parajó (ED481D 2023/014) thanks the I2C postdoctoral Program of the Xunta de Galicia, for their support in funding the study. The authors are also grateful to the research support services of the Universidade de Vigo (CACTI) for the NMR and MS divisions.

Funding Open Access funding provided thanks to the CRUE-CSIC agreement with Springer Nature.

References

1. Plechkova NV, Seddon KR. Applications of ionic liquids in the chemical industry. Chem Soc Rev. 2008;37:123–50. https://doi.org/10.1039/B006677J.
2. Ren F, Wang J, Xie F, Zan K, Wang S, Wang S. Applications of ionic liquids in starch chemistry: a review. Green Chem. 2020;22:2162–83. https://doi.org/10.1039/C9GC03738A.
3. Rogers RD, Seddon KR. Ionic Liquids - Solvents of the Future? Science. 1979;2003(302):792–3.

4. Petkovic M, Seddon KR, Rebelo LPN, Pereira CS. Ionic liquids: a pathway to environmental acceptability. Chem Soc Rev. 2011;40:1383–403. https://doi.org/10.1039/c004968a.
5. Parajó JJ, Villanueva M, Otero I, Fernández J, Salgado J. Thermal stability of aprotic ionic liquids as potential lubricants. Comparison with synthetic oil bases. J Chem Thermodyn. 2018;116:185–96.
6. Salgado J, Parajó JJ, Villanueva M, Rodríguez JR, Cabeza O, Varela LM. Liquid range of ionic liquid – metal salt mixtures for electrochemical applications. J Chem Thermodyn. 2019;134:164–74.
7. Watanabe M, Thomas ML, Zhang S, Ueno K, Yasuda T, Dokko K. Application of ionic liquids to energy storage and conversion materials and devices. Chem Rev. 2017;117:7190–239. https://doi.org/10.1021/acs.chemrev.6b00504.
8. Markiewicz R, Klimaszyk A, Jarek M, Taube M, Florczak P, Kempka M, et al. Influence of alkyl chain length on thermal properties, structure, and self-diffusion coefficients of alkyltriethylammonium-based ionic liquids. Int J Mol Sci. 2021. https://doi.org/10.3390/ijms22115935.
9. Greaves TL, Weerawardena A, Fong C, Krodkiewska I, Drummond CJ. Protic ionic liquids: solvents with tunable phase behavior and physicochemical properties. J Phys Chem B. 2006;110:22479–87. https://doi.org/10.1021/jp0634048.
10. Parajó JJ, Santiago-Alonso A, Vallet P, Teijeira T, Emeterio RS, Villanueva M, et al. comprehensive analysis of the acute toxicity of ionic liquids using microtox® bioassays. Appl Sci. 2024;14:24–80. https://doi.org/10.3390/app14062480.
11. Yalcin D, Christofferson AJ, Drummond CJ, Greaves TL. Solvation properties of protic ionic liquid–molecular solvent mixtures. Phys Chem Chem Phys. 2020;22:10995–1011. https://doi.org/10.1039/D0CP00201A.
12. Vallet P, Bouzón-Capelo S, Méndez-Morales T, Gómez-González V, Arosa Y, de la Fuente R, et al. On the physical properties of mixtures of nitrate salts and protic ionic liquids. J Mol Liq. 2022;350:118483.
13. Thuy Pham TP, Cho C-W, Yun Y-S. Environmental fate and toxicity of ionic liquids: a review. Water Res. 2010;44:352–72.
14. Ibrahim M, Mutalib A, Mutalib A. Ecotoxicity of and Ionic Liquids Towards Vibrio fischeri : Experimental and QSAR Studies. In: Handy S, editor. Progress and Developments in Ionic Liquids. INTECH; 2017. p. 429–49.
15. Parajó JJ, Vallet P, Guimarey MJG, Santiago A, Teijera T, Amigo A, et al. Thermophysical properties of n-alkyl-ammonium nitrate ionic liquids (n = 2,3,4) pure and water saturated for energy applications. J Therm Anal Calorim. 2023;148:6699–714. https://doi.org/10.1007/s10973-023-12194-1.
16. Parajó JJ, Teijeira T, Fernández J, Salgado J, Villanueva M. (2017) Thermal stability of some imidazolium [NTf_2] ionic liquids Isothermal and dynamic kinetic study through thermogravimetric procedures. Journal of Chemical Thermodynamics. https://doi.org/10.1016/j.jct.2017.04.016
17. Parajó JJ, Villanueva M, Sánchez PB, Salgado J. Liquid window of some biologically-active ionic liquids. J Chem Thermodyn. 2018;126:1–10. https://doi.org/10.1016/j.jct.2018.06.014.
18. Salgado J, Villanueva M, Parajó JJ, Fernández J. Long-term thermal stability of five imidazolium ionic liquids. J of Chem Thermodyn. 2013. https://doi.org/10.1016/j.jct.2013.05.049.
19. Salgado J, Parajó JJ, Fernández J, Villanueva M. Long-term thermal stability of some 1-butyl-1-methylpyrrolidinium ionic liquids. J Chem Thermodyn. 2014. https://doi.org/10.1016/j.jct.2014.03.030.
20. Lugo L, Segovia JJ, Martín MC, Fernández J, Villamañán MA. An experimental setup for isobaric heat capacities for viscous fluids at high pressure: squalane, bis(2-ethylhexyl) sebacate and bis(2-ethylhexyl) phthalate. J Chem Thermodyn. 2012;49:75–80. https://doi.org/10.1016/j.jct.2012.01.011.
21. de Sousa C, Marques MA, Guimarey MJG, Domínguez-Arca V, Amigo A, Fernández J. Heat capacity, density, surface tension, and contact angle for polyalphaolefins and ester lubricants. Thermochim Acta. 2021. https://doi.org/10.1021/acs.jced.7b00170.
22. Cerdeiriña CA, Míguez JA, Carballo E, Tovar CA, De La Puente E, Romaní L. Highly precise determination of the heat capacity of liquids by DSC: calibration and measurement. Thermochim Acta. 2000;347:37–44. https://doi.org/10.1016/S0040-6031(99)00414-1.
23. Parajó JJ, Macário IPE, De Gaetano Y, Dupont L, Salgado J, Pereira JL, et al. Glycine-betaine-derived ionic liquids: synthesis, characterization and ecotoxicological evaluation. Ecotoxicol Environ Saf. 2019. https://doi.org/10.1016/j.ecoenv.2019.109580.
24. Parajó JJ, Vallet P, Varela LM, Villanueva M, Salgado J. Ecotoxicity of binary mixtures of ILs and inorganic salts of electrochemical interest. Environ Sci Pollut Res. 2021. https://doi.org/10.1007/s11356-021-17515-1.
25. Han Q, Broomhall HC, Veríssimo NV, Ryan TM, Drummond CJ, Pereira JFB, et al. Protic ionic liquid cation alkyl chain length effect on lysozyme structure. Molecules. 2022. https://doi.org/10.3390/molecules27030984.
26. Gontrani L, Leonelli F, Campetella M. An X-ray and computational study of liquid pentylammonium nitrate. Chem Phys Lett. 2017;687:38–43. https://doi.org/10.1016/j.cplett.2017.08.068.
27. Moshikur RM, Chowdhury MR, Wakabayashi R, Tahara Y, Moniruzzaman M, Goto M. Ionic liquids with methotrexate moieties as a potential anticancer prodrug: Synthesis, characterization and solubility evaluation. J Mol Liq. 2019;278:226–33. https://doi.org/10.1016/j.molliq.2019.01.063.
28. Gómez E, Calvar N, Domínguez Á. Thermal behaviour of pure ionic liquids. In: Handy S, editor. Ionic Liquids. Rijeka: IntechOpen 2015. pp. 199–228; https://doi.org/10.5772/59271
29. Lorenzo M, Vilas M, Verdía P, Villanueva M, Salgado J, Tojo E. Long-term thermal stabilities of ammonium ionic liquids designed as potential absorbents of ammonia. RSC Adv. 2015;5:41278–84. https://doi.org/10.1039/C5RA03192C.
30. Abe H, Takekiyo T, Yoshimura Y, Shimizu A, Ozawa S. Multiple crystal pathways and crystal polymorphs in protic ionic liquids. J Mol Liq. 2018;269:733–7. https://doi.org/10.1071/CH18368.
31. Rodrigues ASMC, Santos LMNBF. Nanostructuration effect on the thermal behavior of ionic liquids. ChemPhysChem. 2016. https://doi.org/10.1002/cphc.201501128.
32. Appetecchi GB, Montanino M, Zane D, Carewska M, Alessandrini F, Passerini S. Effect of the alkyl group on the synthesis and the electrochemical properties of N-alkyl-N-methyl-pyrrolidinium bis(trifluoromethanesulfonyl)imide ionic liquids. Electrochim Acta. 2009;54:1325–32. https://doi.org/10.1016/J.ELECTACTA.2008.09.011.
33. Greaves TL, Drummond CJ. Protic ionic liquids: properties and applications. Chem Rev. 2008. https://doi.org/10.1021/cr068040u.
34. Jeremias S, Carewska M, Conte L, Passerini S, Appetecchi GB. Asymmetry effect of novel per(fluoroalkylsulfonyl)imide anions in pyrrolidinium ionic liquids. RSC Adv. 2013;3:17755–61. https://doi.org/10.1039/C3RA42980F.
35. Bagno A, Butts C, Chiappe C, D'Amico F, Lord JCD, Pieraccini D, et al. The effect of the anion on the physical properties of trihalide-based N. N-dialkylimidazolium ionic liquids Org Biomol Chem. 2005;3:1624–30. https://doi.org/10.1039/b502654g.
36. Machanová K, Wagner Z, Andresová A, Rotrekl J, Boisset A, Jacquemin J, et al. Thermal properties of alkyl-triethylammonium bis{(trifluoromethyl)sulfonyl}imide ionic liquids. J Solution Chem. 2015;44:790–810. https://doi.org/10.1007/s10953-015-0323-3.
37. Wooster TJ, Johanson KM, Fraser KJ, MacFarlane DR, Scott JL. Thermal degradation of cyano containing ionic liquids. Green Chem. 2006;8:691–769. https://doi.org/10.1039/B606395K.

38. Serra PBP, Ribeiro FMS, Rocha MAA, Fulem M, Růžička K, Coutinho JAP, et al. Solid-liquid equilibrium and heat capacity trend in the alkylimidazolium PF6 series. J Mol Liq. 2017;248:678–87. https://doi.org/10.1016/j.molliq.2017.10.042.
39. Lopes JM, Paninho AB, Môlho MF, Nunes AVM, Rocha A, Lourenço NMT, et al. Biocompatible choline based ionic salts: solubility in short-chain alcohols. J Chem Thermodyn. 2013;67:99–105. https://doi.org/10.1016/j.jct.2013.07.025.
40. Fredlake CP, Crosthwaite JM, Hert DG, Aki SNVK, Brennecke JF. Thermophysical properties of imidazolium-based ionic liquids. J Chem Eng Data. 2004;49:954–64. https://doi.org/10.1021/JE034261A.
41. Salgado J, Teijeira T, Parajó JJ, Fernández J, Troncoso J. Isobaric heat capacity of nanostructured liquids with potential use as lubricants. J Chem Thermodyn. 2018;123:107–16. https://doi.org/10.1016/j.jct.2018.03.031.
42. Rocha MAA, Bastos M, Coutinho JAP, Santos LMNBF. Heat capacities at 298.15 K of the extended [CnC1im][Ntf2] ionic liquid series. J Chem Thermodyn. 2012. https://doi.org/10.1016/j.jct.2012.04.025.
43. Gardas RL, Coutinho JAP. A group contribution method for heat capacity estimation of ionic liquids. Ind Eng Chem Res. 2008;47:5751–7. https://doi.org/10.1021/ie800330v.
44. Liaqat S, Shahin MB, Nancarrow P, Zeinab S, Ibrahim T, Abdeljabbar N, et al. Prediction of liquid phase heat capacity of ionic liquids comparison of existing methods and development of new hybrid group contribution models. Ind Eng Chem Res. 2023;62:16093–160112. https://doi.org/10.1021/acs.iecr.3c00675.
45. Dong Q, Muzny CD, Kazakov A, Diky V, Magee JW, Widegren JA, et al. ILThermo: a free-access web database for thermodynamic properties of ionic liquids. J Chem Eng Data. 2007;52(4):1151–9.
46. Montalbán MG, Hidalgo JM, Collado-González M, Díaz Baños FG, Víllora G. Assessing chemical toxicity of ionic liquids on vibrio fischeri: correlation with structure and composition. Chemosphere. 2016;155:405–14.
47. Stolte S, Matzke M, Arning J, Böschen A, Pitner W-R, Welz-Biermann U, et al. Effects of different head groups and functionalised side chains on the aquatic toxicity of ionic liquids. Green Chem. 2007;9:1170–9. https://doi.org/10.1039/B711119C.
48. Silva FA, Coutinho JAP, Ventura SPM. Aquatic toxicology of ionic liquids (ILs) in encyclopedia of ionic liquids. 1° Edition. Springer Nature 2019. pp. 117–33.
49. Ventura SPM, Gonçalves AMM, Sintra T, Pereira JL, Gonçalves F, Coutinho JAP. Designing ionic liquids: the chemical structure role in the toxicity. Ecotoxicology. 2013;22:1–12. https://doi.org/10.1007/s10646-012-0997-x.
50. Ventura SPM, Esilva FA, Gonçalves AMM, Pereira JL, Gonçalves F, Coutinho JAP. Ecotoxicity analysis of cholinium-based ionic liquids to Vibrio fischeri marine bacteria. Ecotoxicol Environ Saf. 2014;102:48–54. https://doi.org/10.1016/j.ecoenv.2014.01.003.
51. Zhao D, Liao Y, Zhang Z. Toxicity of ionic liquids. Clean (Weinh). 2007;35:42–8. https://doi.org/10.1002/clen.200600015.
52. Docherty KM, Kulpa CF. Toxicity and antimicrobial activity of imidazolium and pyridinium ionic liquids. Green Chem. 2005;7:185–9. https://doi.org/10.1039/B419172B.
53. Biczak R, Pawłowska B, Bałczewski P, Rychter P. The role of the anion in the toxicity of imidazolium ionic liquids. J Hazard Mater. 2014;274:181–90. https://doi.org/10.1016/j.jhazmat.2014.03.021.
54. Garcia MT, Gathergood N, Scammells PJ. Biodegradable ionic liquids part II effect of the anion and toxicology green chemistry. Royal Society of Chemistry. 2005. https://doi.org/10.1039/B411922C.
55. Cvjetko Bubalo M, Radošević K, Radojčić Redovniković I, Halambek J, Gaurina SV. A brief overview of the potential environmental hazards of ionic liquids. Ecotoxicol Environ Saf. 2014. https://doi.org/10.1016/j.ecoenv.2013.10.019.